BEAM TESTS OF THE CLEO III LIF-TEA RING IMAGING CHERENKOV DETECTOR

M. Artuso, F. Azfar, A. Efimov, S. Kopp, R. Mountain, S. Schuh, T. Skwarnicki, S. Stone, and G. Viehhauser*
Syracuse University, Syracuse, NY 13244-1130

and

T. Coan, V. Fadeyev, I. Volobouev, and J. Ye†
Southern Methodist University, Dallas, TX 75275-0175

and

S. Anderson, Y. Kubota, and A. Smith†
University of Minnesota, Minneapolis, MN 55455-0112

and

E. Lipeles†
California Institute of Technology, Pasadena, CA 91125-0001

ABSTRACT

We present preliminary results from a test beam run of CLEO III RICH modules. The system consists of LiF radiators and multiwire proportional chambers containing a mixture of CH_4 and TEA gases. The radiators were both flat and "sawtooth." The data were taken in a beam dump at Fermilab. We will discuss the chamber stability, electronics, the number of photons observed for both radiators, the angular resolution per photon and the angular resolution per track.

*Supported by National Science Foundation.
†Supported by Dept. of Energy

1 Description of the CLEO III RICH System

The CLEO III RICH is based on the 'proximity focusing' approach, in which the Cherenkov cone is simply let to expand in a volume filled with gas transparent to ultraviolet (UV) light before intersecting the detector surface where the coordinates of the Cherenkov photons are reconstructed. The components of our system are illustrated in Fig. 1. They consist of a LiF radiator, providing UV photons, an expansion region, and a photosensitive detector. The angle θ_p is the polar angle of the incident particle with respect to the radiator normal, θ is the Cherenkov angle and ϕ specifies the azimuthal angle of the Cherenkov photons. Our system is based on the one developed by the College de France-Strasbourg group [1].

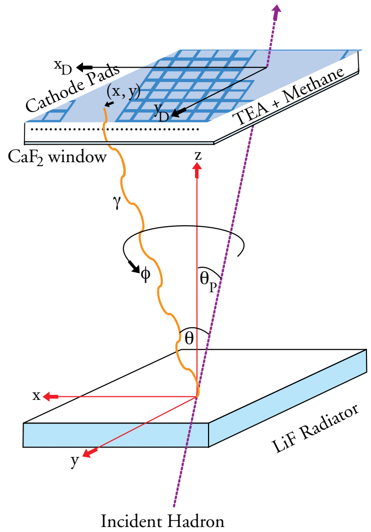

Figure 1: Schematic diagram of LiF-TEA RICH system.

The photosensitive detector is really the starting point for the system design. We chose a multiwire proportional chamber filled with a mixture of Triethylamine (TEA) gas and Methane because it has good quantum efficiency (up to 35%) in a narrow wavelength interval between 135-165 nm, and an absorption length of only 1/2 mm. Other choices such as TMAE gas or phototubes would have taken most of our allotted 16 cm of radial space, and thus not allowed a full size detector to be constructed. Other solutions such as DIRC [2] were not feasible due to the existing detector iron and the desire to limit the detector thickness to less than 12% of a radiation length.

The position of Cherenkov photons is measured by sensing the induced charge on array of 7.6 mm x 8.0 mm pads. Since the pulse height distribution from single photons is exponential, this requires the use of low noise electronics. A dedicated VLSI chip, called VA_RICH, based on a very successful chip developed for solid state applications, has been designed and produced for our application at IDE AS, Norway. We have fully characterized hundreds of 64 channel chips, mounted on hybrid circuits. For moderate values of the input capacitance C_{in} the equivalent noise charge measured ENC is found to be about:

$$ENC = 130e^{-} + (9e^{-}/pF) \times C_{in} \quad . \tag{1}$$

Its dynamic range is between 450,000 and 900,000 electrons, depending upon whether we choose a bias point for the output buffer suitable for signals of positive or negative polarity or we shift this bias point to have the maximum dynamic range for signals of a single polarity.

Two VA_RICH chips are mounted on a hybrid circuit. These are attached via miniature connectors to the back of the cathode board of the photon detectors. We group 5 hybrids (10 chips) into a single readout cell cabled to data boards located in VME crates just outside the detector cylinder. Chips in the same readout cell share the same control signals and bias lines from the data boards and output lines from the hybrid to the detector.

The analog output of the VA_RICH is transmitted to the data boards as a differential current, transformed into a voltage by transimpedance amplifiers and digitized by a 12 bit differential ADC. These receivers are part of complex data boards which perform several important analog and digital functions. Each board contains 15 digitization circuits and three analog power supply sections providing the voltages and currents to bias the chips, and calibration circuitry. The digital component of these boards contains a sparsification circuit, an event buffer, memory to store the pedestal values, and the interface to the VME cpu.

If a track is incident normal to a LiF radiator no light is emitted in the wavelength range that can be detected by TEA, due to total internal reflection. A full system for CLEO, therefore, would require that the radiators be tilted until the track angles are about 15°. This causes several serious problems. One is the difficulty in accurate radiator mounting. More importantly, some of the light from one radiator must traverse through another radiator resulting in lost light and reconstruction problems. To eliminate these problems a novel radiator geometry has been proposed [3]. It involves cutting the outer surface of the radiator with a profile resembling the teeth of a saw, and therefore it is referred to as a "sawtooth radiator" [3]. The major advantage of this configuration is that it reduces the losses of photons due to total internal reflection at the interface between the radiator and the expansion region. It also turns out that the angular resolution per photoelectron is greatly decreased [4].

A crystal profile with teeth about 4 mm deep in a plate of 12 mm thickness is a good compromise between uniformity in light output, and cost. A detailed simulation has shown that a tooth angle of 42° is close to optimal and technically feasible. Fig. 2 summarizes the results of this study, which focuses on particles with $p = 2.8$ GeV/c. The mean number of reconstructed photoelectrons, N_{pe}, Cherenkov angle resolution per photon, Cherenkov angle resolution per track, and the probability for a π to fake a K are plotted as a function of the angle θ between the charged particle and the normal to the radiator inner surface.

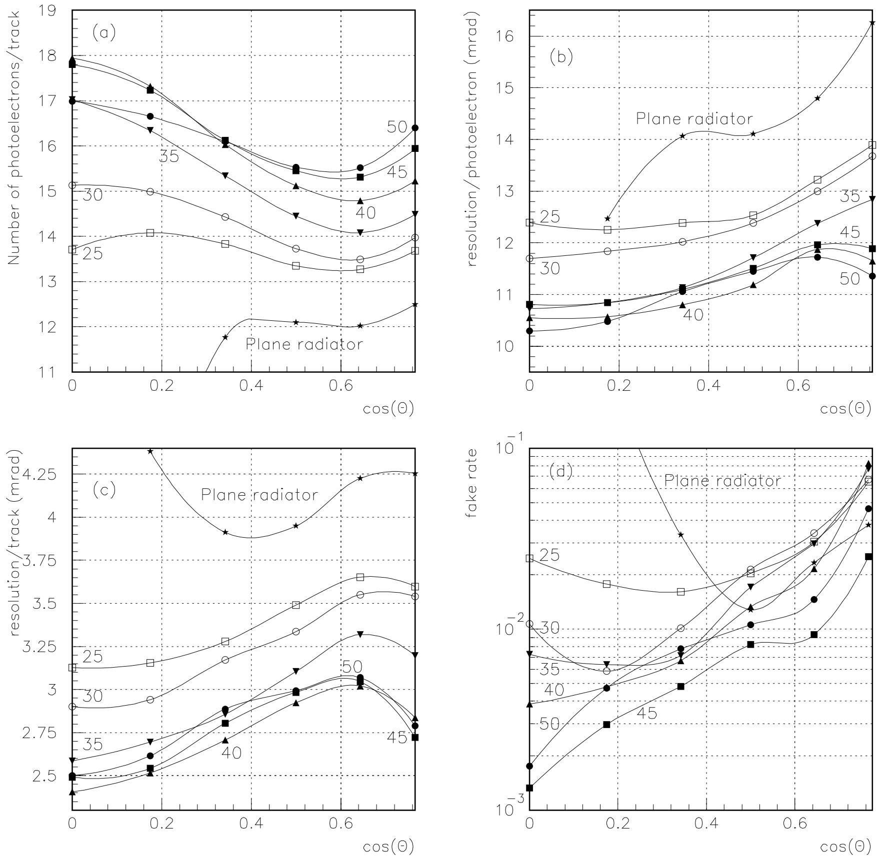

Figure 2: Performance of the sawtooth radiator as a function of the incident track angle. (Normal incidence is described by $\cos(\theta)$ of 0.) The curves are parametrized by the sawtooth angle: (a) The average number of detected photoelectrons, (b) The angular resolution per photon, (c) the angular resolution per track as a function of incident track angle, (d) the probability for a 2.8 GeV/c π to fake a K for 95% π detection efficiency.

The fake rates shown in Fig. 2(d) can be estimated accurately for the plane radiator by using the 12.8 mr Cherenkov angle separation coupled with the estimated resolution per track. However, such a procedure is far too optimistic in the case of the sawtooth radiator. The cause of the worsening of the fake rate is the that the image pattern of the photons is not described by a single curve as in the case of the plane radiator. In fact the image has two main branches and two secondary branches which contain <10% of the photons. The predicted image pattern for tracks normally incident on a sawtooth is shown in Fig. 3. The possibility for multiple interpretations of a photon path is responsible for the worsening of the fake rate. In the data analyzed here only the two main branches are considered.

There are several problems inherent in producing such radiators, including the ability to precisely cut the LiF without cleaving the material and the ability to polish the surface to yield good

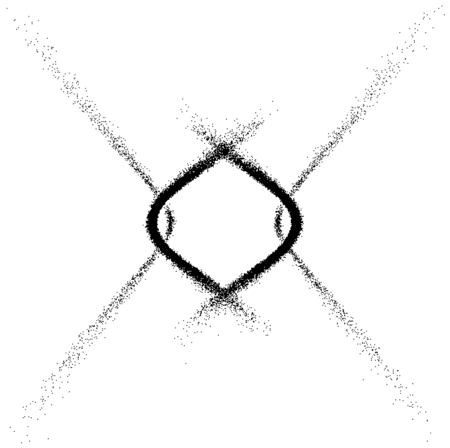

Figure 3: Cherenkov photon pattern on the detector plane for a track at normal incidence to a sawtooth radiator. The lense densely populated paths result from a combination of one refraction and one reflection.

ultraviolet light transmission. Furthermore, the production time and cost need to be reasonable. We worked with OPTOVAC in North Brookfield Mass. to produce two full sized radiators. A close up of two sawtooth radiators separated by a plane radiator is shown in Fig. 4.

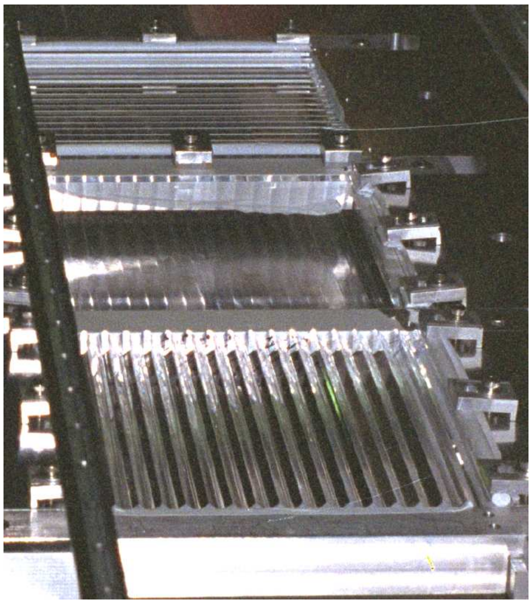

Figure 4: Two sawtooth radiators separated by a plane radiator. The teeth are aligned perpendicular to one other in this test beam setup.

Transparency measurements for the two sawtooth radiators have been made relative to a plane polished sample of LiF. The transmissions for both pieces are very good. One exceeded the normally polished sample by 10% while the other was equal to it. The measurements for the better sample are shown in Fig. 5.

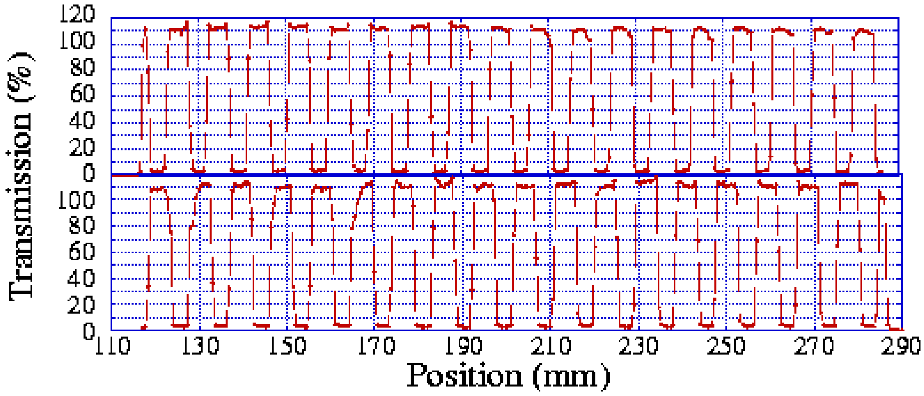

Figure 5: Optical transmission of prototype sawtooth radiator relative to a 45° prism polished with conventional techniques at 157 nm. The top curve is for the left side of the 19 teeth and the bottom curve is for the right side.

A sketch of a photon detector module is shown in Fig. 6. The MWPC anode wires run the

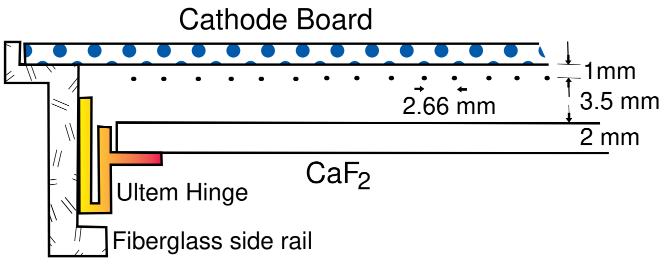

Figure 6: A cross-section of one RICH photon detection module.

entire length of the detector, approximately 2.5 m. They are supported every 30 cm by a ceramic spacer. The CaF_2 window joints are placed directly on top of these spacers to minimize the loss of photon acceptance.

A fully constructed module RICH photon detector module is shown in Fig. 7. It is mounted on a strongback, which is removed after assembly into the chamber holding structure. Construction of these chambers proceeded after successful prototype testing [5].

2 Test Beam Results

Two completed CLEO III RICH modules were taken to Fermilab and exposed to high energy muons (> 100 GeV$/c$) emerging from a beam dump. The modules were mounted in a leak tight aluminum box with exactly the same scheme as we will use in the final detector. Two sets of wire chambers were set up in the beam line to provide track direction and there were scintillators to provide a trigger. The data acquisition system was a prototype for the final CLEO system.

Figure 7: One of the 30 needed photon detector modules.

Beam conditions were much worse than expected. The particle flux was ten times higher than anticipated, due in large part to the experimenters in front of us lowering their magnetic field. In addition there was a large neutron background. We survived by receiving dedicated beam time at much lower intensity. Still the background conditions and particle fluxes are much higher than we expect in CLEO by about two orders of magnitude and we don't expect significant neutron background in CLEO.

For this test we read out every channel in every event. This proved to be quite useful because we found a rather large coherent noise component of about 1000 electrons whose source was imperfect grounding of the system and noisy switched power supplies in the DAQ crates. (These will be replaced in the final system.) However, we removed virtually all of the coherent noise by averaging the non-hit channels on each hybrid card and generating an event-by-event pedestal correction. We became so enamored of this procedure that we are adapting it in the final CLEO data boards. Thus our final noise value is approximately 400 e^- r.m.s. per channel. Furthermore, this trick will probably be used to lower noise in the CsI calorimeter system and will possibly be used for the silicon vertex detector.

The pulse-height distribution of candidate photon pad clusters after a 5σ cut above the noise is shown in Fig. 8(a). The distribution has been background subtracted. The pulse-heights follow an exponential distribution as expected. Fitting the slope provides a measurement of the gain; actually the fraction of the gain seen on the pad plane. We call this the pad gain. The pulse-height distribution for the charge tracks is much higher.

The number of observed photons as a function of pad gain, uncorrected for background, is shown in Fig. 8(b). Our operating point for these tests is a pad gain of about 40,000 and is on plateau.

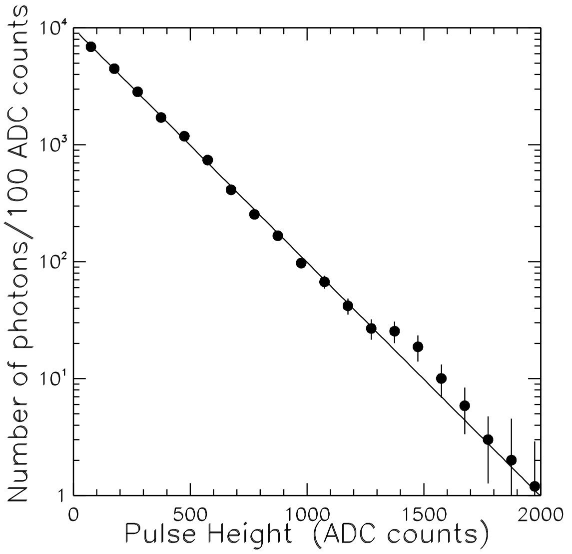

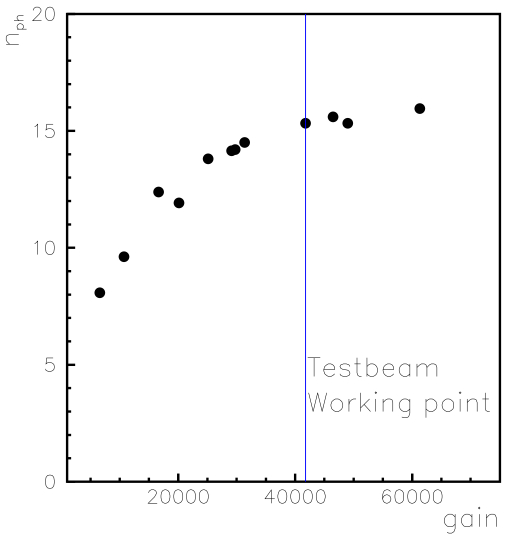

Figure 8: (a)The pulse height distribution for hits 5σ above noise from photon candidate clusters. (b) The number of observed photons, including background, as a function of pad gain.

For the plane radiator, we were able to configure the detector so that the photon pattern would appear only in one chamber. For the sawtooth radiator we would have needed three chambers to fully contain the image. Sample images from the plane and sawtooth radiators are shown in Fig. 9. Here the track was incident at 30° to the plane radiator and zero degrees for the sawtooth.

The best way to ascertain the expected performance is to first view the number of photons and the angular resolution per photon. In Fig. 10(left) we show the Cherenkov angle for all photons from many tracks. Fitting to a Gaussian with an asymmetric tail and quadratic background gives an angular resolution per photon of about 13.5±0.2 mr and a background of 8.8%. The asymmetric tail is due to the chromatic error [7].

Our Monte Carlo simulation includes information on CH_4-TEA quantum efficiency as a function of wavelength, crystal transmissions, etc... The background under the single photon peak has been modeled and included in our simulation. We think the background is mostly due to out of time tracks and that the background level in CLEO will be much smaller. The Monte Carlo simulation is in good agreement with the angular resolution per photon, and, after being adjusted to yield more photons, is also in good agreement with the photon distribution. From these data we can estimate the expected resolution per track, and compare to what we measure. The results presented here are preliminary; we have more data to analyze and the reconstruction algorithms are undergoing improvement.

Fig. 10(right) shows the number of detected photons per track, before background subtraction. The average number, after background subtraction, is approximately 14. Including some smearing from the background, we estimate the final average resolution per track to be 3.9 mr. However,

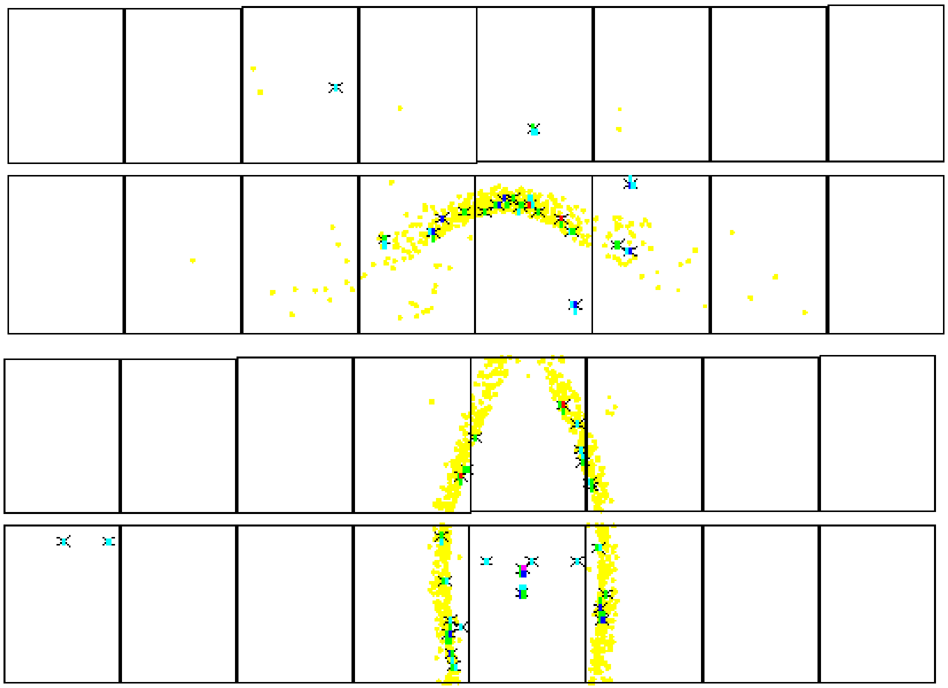

Figure 9: Single event images from the plane (top) and sawtooth (bottom) radiators. The light yellow points are where photons are expected to hit the detector plane. The green and blue points are photon hits and the crosses mark the reconstructed photon positions. The red point between the two arcs of the lower images shows the charged track impact point.

we have not included any error from the tracking system. Monte Carlo simulation of our tracking system shows that it contributes a 2.3 mr r.m.s. error [6]. Thus we expect a resolution of 4.5 mr on the Cherenkov angle per track, which is what we observe in Fig. 11. Most of the tracking error contribution comes from inaccurate prediction of the impact point of the track on the radiator, rather than a poorly determined track angle. We expect this to be substantially better in CLEO III, and thus expect to achieve our goal of 4.2 mr resolution. The pion momentum distribution from $B^o \to \pi^+\pi^-$ is a box shaped spectrum from 2.5 to 2.8 GeV/c, spread by the Doppler shift due to the B momentum. The angular separation between K and π at 2.8 GeV/c is 12.8 mr. Thus 4.2 mr resolution will provide better than 3σ K/π separation for all B decays [8].

In Fig. 12 and Fig. 13 we show similar plots for the sawtooth radiator. We see the expected improvement in angular resolution per photon of 11.8±0.2 mr. Here the Monte Carlo predicts a slightly better resolution. The number of observed photons is approximately 13.5. The measured Cherenkov angular resolution per track is 4.8±0.05 mr. The Monte Carlo prediction is 4.1 mr. We are not sure of the sources of this disagreement but it is possible that the crystal alignment is not adequate or that we do not know the sawtooth angle precisely enough. The number of photons needs to be corrected upwards by a factor of 1.7 since we do not have complete acceptance for

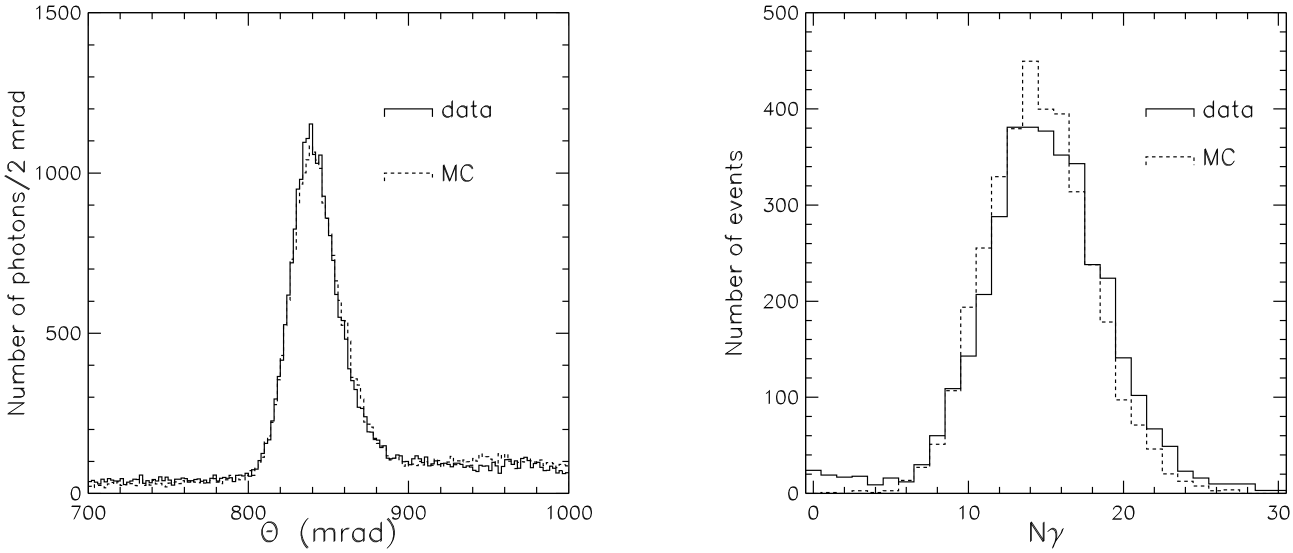

Figure 10: Results from test beam studies compared with Monte Carlo simulation for a plane radiator with tracks at 30° incidence. (left) The Cherenkov angle of each photon for a sum over many tracks. (right) The number of photons for each track.

both branches of the sawtooth image. For full acceptance we calculate 20 photons on average, after removing the 9% background. The sawtooth radiators work and we will use them for 3/7 of the detector, which covers 5/8 of the available solid angle.

3 Conclusions

Fig. 14 shows the measured resolution per track for the plane and sawtooth radiators as a function of the background subtracted number of photons detected. The curves are fits to the parameterization $(a/\sqrt{n})^2 + b^2$. Unfortunately, the parameters a and b have no relevant meaning since their errors are completely anti-correlated.

Table 1 summaries the achieved and predicted track resolutions.

Table 1: Track resolutions (mr)

Radiator	Data	Monte Carlo†	MC no background & no tracking errors	CLEO expectations
plane (30°)	4.5±0.07	4.5	3.9	4.0
sawtooth (0°)	4.8±0.05	4.1	3.8	2.9-3.8

† Statistical errors on the Monte Carlo samples are ±0.04 mr.

These data though preliminary show that we have a good understanding of the system and

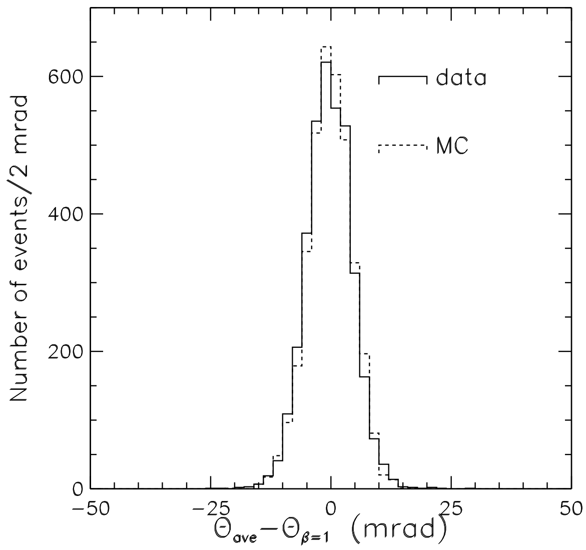

Figure 11: The Cherenkov angular resolution per track for a plane radiator with tracks at 30° incidence.

we can expect the predicted levels of efficiency versus rejection in CLEO III. Furthermore, the chambers held voltage, the electronics functioned, and the gas system worked, in much more difficult environment than will be present in CLEO. We have data for several additional incident angles for both plane and sawtooth radiators. After we have analyzed these data and understood the systematic errors in more detail, we will present more complete results in a later publication.

4 Acknowledgments

We thank Fermilab for their cooperation in providing a high energy particle beam and computing. Especially noteworthy for their help were Chuck Brown and Joel Butler. Franz Muheim and Stephen Playfer played major roles in the early stages of this work. Jacques Seguinot and Tom Ypsilantis provided initial insights and encouragement. We appreciate the help of our CLEO colleagues, especially Chris Bebek, Jeff Cherwinka, Charlie Strohman and Frank Wurthwein. Support was provided by the National Science Foundation and the Department of Energy.

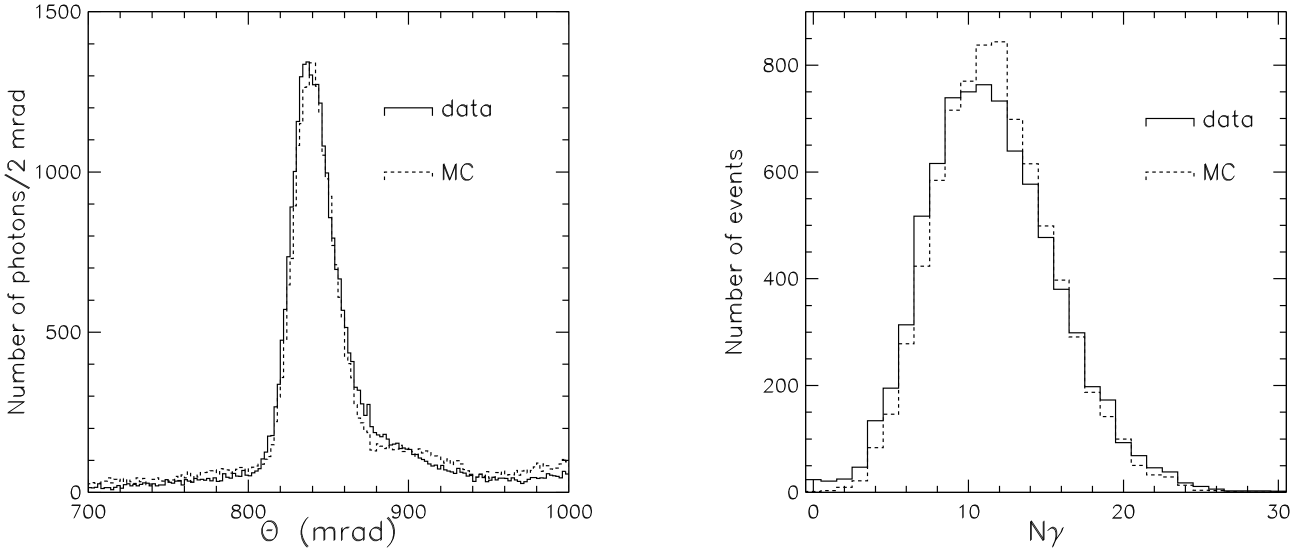

Figure 12: Results from test beam studies compared with Monte Carlo simulation for a sawtooth radiator with tracks at normal incidence. (left) The Cherenkov angle of each photon for a sum over many tracks. (right) The number of photons for each track.

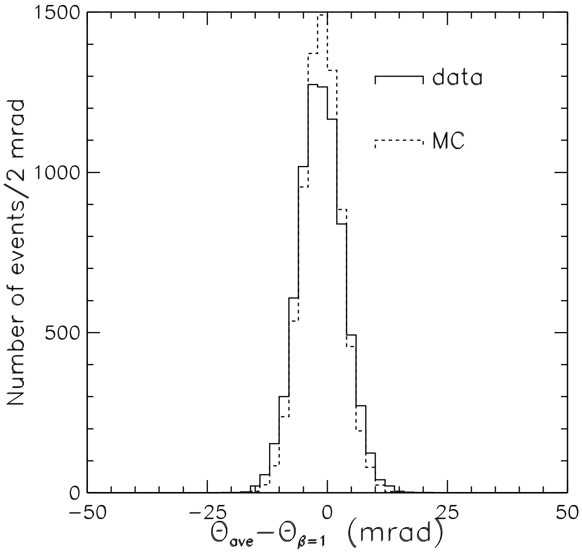

Figure 13: The Cherenkov angular resolution per track for a sawtooth radiator with tracks at normal incidence.

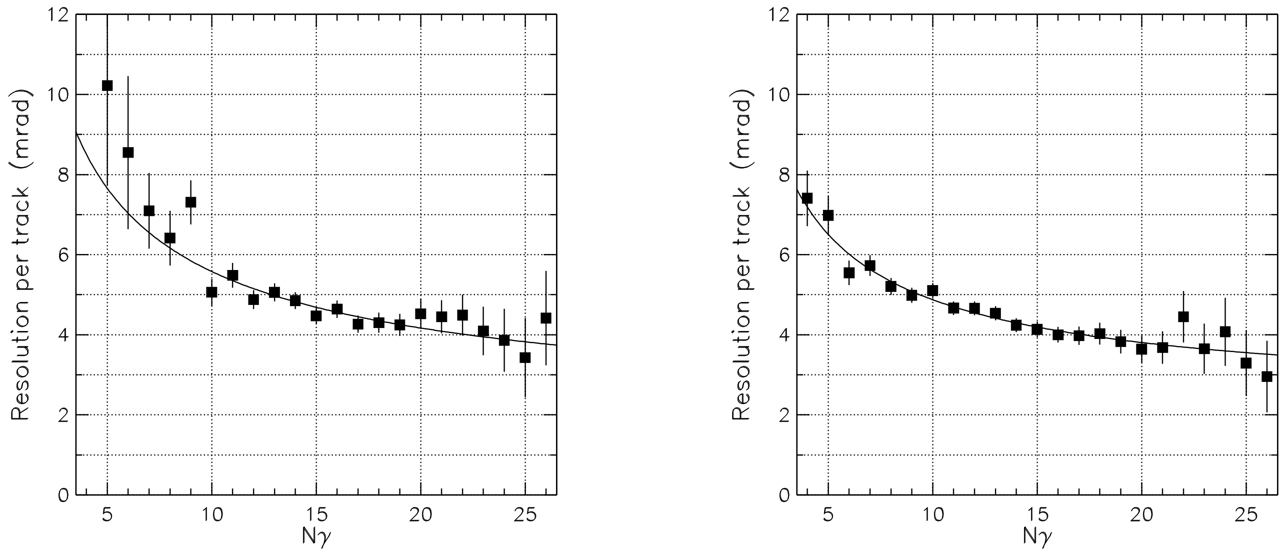

Figure 14: The Cherenkov angular resolution per track as a function of the number of detected photons (background subtracted) for a plane radiator with tracks at 30° incidence (left) and for a sawtooth radiator with tracks at normal incidence (right).

References

[1] R. Arnold *el al.*, *Nucl. Inst. and Meth.* **A314** (1992) 465.

[2] B. Ratcliff, *Nucl. Instr. and Meth.* **A343** 292 (1994).

[3] A. Efimov *et al.*, *Nucl. Instr. and Meth.* **A365** 285 (1995).

[4] The improvement in angular resolution per photon is due to the reduced refraction at the LiF-N_2 interface. Thus the angular spread due to chromatic dispersion is not magnified as much for the sawtooth radiator as it is for the plane radiator.

[5] S. Playfer *et al*, *Nucl. Instr. and Meth.* **A371** 321 (1996).

[6] We used 30 cm^2 wire chambers borrowed from Fermilab which had 5 mm wide cells. We equipped the wire readout with TDC's, also borrowed from Fermilab, but have not implemented the TDC readout. If time permits we can, in principle, improve the tracking errors.

[7] We have not quoted systematic errors on the various measured resolutions in this paper. The systematic errors are likely to be as large if not larger than the statistical errors, and thus we emphasize the preliminary nature of these results.

[8] We also expect to have 2σ π/K separation at 2.8 GeV/c from the dE/dx system in the drift chamber.